0.4%) and a trace of anisole (0.2%). The 2,6-xylenol was separated from the mixture by fractional distillation, followed by multiple recrystallizations and then medium-pressure liquid chromatography. The purity of the final product was determined by gas chromatography to be 99.9%.

The quantity and location of the deuterium in the 2,6-xylenol were determined by ^{1}H NMR spectroscopy. The spectrum was measured in the presence of an internal standard (*sym*-trioxane). The quantity of methyl protons (0.46 at 2.20 ppm) showed that 92 atom % substitution of deuterium on the methyl groups had occurred. No para-substituted hydrogen was observed, indicating complete deuteration at that site. Some of the meta hydrogens (15%) were also absent (1.70 H's at 7.02 ppm). Apparently under the extreme conditions of the alkylation reaction, slow exchange also occurred at this relatively unreactive position. A peak at 5 ppm, due to 0.67 hydroxyl hydrogen, was indicative of exchange at the hydroxyl during the isolation and purification.

The polymerization (reaction 3) was carried out with a copper/diamine catalyst.[4] High molecular weight (intrinsic viscosity in chloroform, 0.57 dL/g; M_w from GPC using poly(phenylene oxide) standards, 43 800 daltons) polymer was obtained in the same reaction time required for polymerization of the nondeuterated monomer. Thus, there is no discernible isotope effect in the polymerization.

The ^{1}H NMR spectrum of the deuterated polymer was measured with *sym*-trioxane present as an internal standard. A weak resonance at 2.05 ppm corresponded to 0.47 methyl H per repeat (92 atom % deuterium on the methyls)—identical with the value for the methyl groups in the monomer. The intensity of the resonance for the aryl hydrogens at 6.48 ppm corresponded to 1.64 hydrogens per repeat unit (18 atom % deuterium on the rings). An increase in deuterium on the ring was expected based on a suggestion[5] that an NIH shift[6] during 2,6-xylenol polymerization can result in a transfer of the hydrogen in the 4-position of monomer to the 3-position of the repeat unit in the polymer.

Acknowledgment. We thank Dr. G. R. Chambers for useful discussions and his help with the high-temperature methylation reaction.

References and Notes

(1) Maconnachie, A.; Kambour, R. P.; White, D. M.; Rostami, S.; Walsh, D. J. *Macromolecules*, following paper in this issue.
(2) Smith, W. E. U.S. Patent 4 048 239, Sept 13, 1977.
(3) Hamilton, S. B. U.S. Patent 3 446 856, May 27, 1969.
(4) Hay, A. S. U.S. Patent 4 028 341, April 7, 1977.
(5) McNelis, E. *J. Org. Chem.* **1966**, *31*, 1255.
(6) Jerina, D. M.; Daly, J. W.; Witkop, B. *J. Am. Chem. Soc.* **1967**, *89*, 3347, 5488.

Temperature Dependence of Neutron Scattering Behavior and Resultant Thermodynamics of Mixing of Poly(2,6-dimethyl-1,4-phenylene oxide) in Polystyrene†

Ann Maconnachie,*‡ Roger P. Kambour,§ Dwain M. White,§ Shamsedin Rostami,‡ and David J. Walsh‡

Polymer Physics and Engineering Branch, Corporate Research and Development, General Electric Company, Schenectady, New York 12301, and Department of Chemical Engineering and Chemical Technology, Imperial College, London SW7 2BY, England.
Received January 4, 1984

ABSTRACT: Small-angle neutron scattering (SANS) measurements have been carried out as a function of temperature on blends of polystyrene with poly(2,6-dimethyl-1,4-phenylene oxide). From the temperature dependence of the interaction parameter, χ_{12}, a negative heat of mixing consistent with calorimetry values and a negative local entropy of mixing are derived. A Θ temperature of 345 °C has been estimated. The spinodal has been simulated from the thermodynamic data and Flory's equation-of-state theory and has been compared with the position of the spinodal estimated from the SANS measurements. Phase separation is predicted to occur above 350 °C.

Introduction

During the past few years a great deal of interest has been shown in the thermodynamics and physical and mechanical properties of polymer blends. It was thought that high molecular weight polymers were basically immiscible but many polymers have now been shown to be miscible.[1]

There is increasing evidence that polymer miscibility can be effected by specific interactions between the polymers. These specific interactions give rise to favorable heats of mixing which dominate any unfavorable noncombinatorial entropy contributions which may arise. One such miscible blend which is of considerable interest is that of polystyrene (PS) with poly(2,6-dimethyl-1,4-phenylene oxide), trivially named poly(xylenyl ether) (PXE), which forms the basis of a set of engineering thermoplastics. All the evidence indicates that PS/PXE blends are miscible in all proportions and over a considerable range of molecular weights.[2-4] Phase separation has not been observed for the pure PS/PXE blends but the addition of a sufficient amount of one of the halogens[5-8] to either the phenyl group of the PS or the phenylene ring of the PXE will cause phase separation. PS/PXE blends have a negative heat of mixing[9] and also a negative volume of mixing,[10] both of which are indicative of a favorable specific interaction. The actual nature of the specific interaction has not been completely elucidated but there is some evidence of an interaction between the phenyl and phenylene rings[3] and

† Presented in part at the American Physical Society Meeting, Los Angeles, CA, March 24, 1983 and at the International Conference on Polymer Blends, Capri, Naples, June 2, 1983.
‡ Imperial College.
§ General Electric Co.

0024-9297/84/2217-2645$01.50/0

Table I

polymer	M_w(GPC)	M_w/M_n
PS	34 000	<1.05
d-PS	33 300	<1.05
PXE	44 000	
d-PXE	37 500[a]	2.23

[a] Measured by low-angle light scattering.

between the methyl groups and the phenyl rings.[11]

Small-angle neutron scattering (SANS) is uniquely suited to explore both the structure and thermodynamics of polymer blends. Using SANS it is possible to measure the single-chain conformation of the components of the blend and also, through the second virial coefficient and thus the Flory–Huggins interaction parameter, to obtain information about the thermodynamics of the blends. Previous SANS measurements by the authors have been carried out on blends of PS with bromine-substituted PXE as a function of bromine content.[8] These experiments indicated that it was possible to predict the critical molecular weight required for phase separation when bromine was present. However, extrapolation of the data on critical bromine levels to infinite molecular weight seemed to show that phase separation would never take place.

One method of obtaining information about the phase behavior of these blends is to measure the temperature dependence of the scattering in the liquid state. Using a PS matrix containing a low concentration of deuterated poly(xylenyl ether) (d-PXE), it is possible to cover a 170 °C temperature range from the glass transition temperature of PS (ca. 100 °C) to the decomposition temperature of d-PXE (ca. 280 °C). This range is sufficiently wide to permit the temperature dependence of the scattering parameters to be determined reasonably accurately, which in turn allows calculations of the thermodynamic quantities of mixing and the Flory Θ temperature. The Flory equation of state can now be applied with these data to calculate the position of the spinodal, which can then be compared with spinodal temperatures obtained by extrapolation to zero of reciprocal scattering intensities at zero angle.

Experimental Section

(1) **Materials.** Polystyrene-d_8 (d-PS) and polystyrene (PS) were obtained from Polymer Laboratories, Church Stretton, England. Poly(2,6-dimethyl-1,4-phenylene oxide) (PXE) and deuterated poly(2,6-dimethyl-1,4-phenylene oxide) (d-PXE) were prepared at General Electric. Details of the preparation of d-PXE by White and Nye are given in a separate paper.[12] The d-PXE has a deuterium/hydrogen ratio of 2.85 as determined by mass spectroscopy. Details of the molecular weights and molecular weight distributions of these polymers are given in Table I.

(2) **Sample Preparation.** In order to keep losses of the d-PXE to a minimum and to make up concentrations which were as accurate as possible, a master batch of d-PXE in PS was prepared which was then diluted to obtain a number of concentrations. The master batch of d-PXE in PS was prepared by dissolving known amounts of the two polymers in chloroform and reprecipitating this mixture in methanol. The resulting fine precipitate was filtered off and dried in a vacuum oven at 60 °C for 24 h. Samples A3 to A6 of d-PXE in PS were obtained by diluting this original mixture (A2) with PS. Because the measurements were to be carried out on samples which were liquid, it was necessary to degas them to eliminate any possibility of bubble formation which would affect the scattering from the samples. Melt mixing could also be carried out at the same time. Appropriate amounts of A2 and then PS were weighed into neutron scattering cells and melted down at about 190 °C. The neutron scattering cells were flat-sided, silica cells with a path length of 2 mm and a total sample volume of approximately 0.6 cm^3. The cells were evacuated and degassed at 280 °C. To aid degassing and to ensure complete mixing, a small metal bar was placed in each cell and this was then used to stir the mixture with the aid of a powerful magnet. Degassing took between 1 and 2 h, depending on the sample. A sample of pure PS (A1S) was similarly prepared. The cells were then sealed under vacuum.

Table II
Sample Composition

sample[a]	matrix polymer	deuterated polymer	wt fraction of deuterated polymer
A1S	PS	d-PXE	0
A2	PS	d-PXE	0.0299
A3	PS	d-PXE	0.0242
A4	PS	d-PXE	0.0200
A5	PS	d-PXE	0.0154
A6	PS	d-PXE	0.0098
Ba1	PXE	d-PS	0
Ba3	PXE	d-PS	0.01033
Ba4	PXE	d-PS	0.01553
Ba5	PXE	d-PS	0.02028
Ba6	PXE	d-PS	0.02500
Bi2	PXE	d-PXE	0.02044
Bh1	PS	d-PS	0
Bh2	PS	d-PS	0.0257

[a] Samples A1S to A6 are collectively referred to as set A.

As the temperature dependence of the scattering was only to be measured for set A, all other samples were compression molded and quenched.

A sample of d-PS in PS (Bh2) was prepared by dissolving the appropriate amounts of the two polymers in 2-butanone and reprecipitating this mixture in methanol. The resulting precipitate was filtered off and dried in a vacuum oven at 60 °C for 24 h. Powders Bh1 and Bh2 were compressed into disks about 1 mm thick, under vacuum, molded at 150 °C, and then cooled below their glass transition temperatures.

Samples of d-PXE in PXE (Bi2) and d-PS in PXE (Ba1–Ba6) were prepared by codissolution in chloroform and reprecipitation in methanol followed by vacuum-drying. Disks of these samples were prepared by compression molding at 260 °C and quenching in water.

Details of all these samples are given in Table II.

(3) **Neutron Scattering Measurements.** Measurements were made on the small-angle scattering instrument, D11, at the Institut Max von Laue-Paul Langevin, Grenoble, France. The sample-to-detector distance was 5.66 m and the neutron wavelength, λ, was 10 Å, giving a q range of 0.033–0.011 Å^{-1} ($q = (4\pi/\lambda) \sin(\theta/2)$, where θ is the scattering angle). Details of SANS measurements have been given elsewhere.[13]

Measurements on the samples of set A were made at eight temperatures between 104 and 274 °C. The sealed silica cells were heated electrically in a brass holder which was double glazed with silica windows. This assembly was placed in an insulated container so that temperature losses were kept to a minimum. The error in the temperature was estimated to be ±1 °C. SANS measurements on all the other samples were carried out at room temperature. No void scattering was observed from set A. Some void scattering, however, was observed from the pure PXE background sample (Ba1).

Theory

(1) **SANS Data Analysis.** The scattered intensity from each polymer mixture was corrected for incoherent scattering by subtracting the scattering from a background sample which contained no deuterated polymer. The incoherent scattering from the small amount of deuterium present in the mixture was considered to be negligible. The scattered intensity was further adjusted for detector efficiency and normalized by using the scattering from water. The final expression for the normalized intensity is

$$I(q) = \frac{I_s}{I_w} \frac{1 - (\mathrm{TRW})}{4\pi d_s (\mathrm{TRS})} g(\lambda) \qquad (1)$$

Table III
Neutron Scattering Lengths, Specific Volumes, and Neutron Contrasts for Various Polymers

T, °C	polymer 2	$10^{12}b_2$, cm	$v_{2,sp}$, cm^3 g^{-1}	polymer 1	$10^{12}b_1$, cm	$v_{1,sp}$, cm^3 g^{-1}	$10^{24}K^2$, cm^2
104	d-PXE	9.071	0.9139	PS	2.328	0.9865	43.330
128	d-PXE	9.071	0.9280	PS	2.328	0.9990	43.241
152	d-PXE	9.071	0.9427	PS	2.328	1.0120	43.149
173	d-PXE	9.071	0.9561	PS	2.328	1.0240	43.072
203	d-PXE	9.071	0.9762	PS	2.328	1.0418	42.955
225	d-PXE	9.071	0.9916	PS	2.328	1.0554	42.866
247	d-PXE	9.071	1.0076	PS	2.328	1.0695	42.776
273	d-PXE	9.071	1.0273	PS	2.328	1.0868	42.666
260	d-PXE	9.071	0.9762	PXE	2.908	0.9762	37.98
100	d-PS	10.656	0.9865	PS	2.328	0.9865	69.36
260	d-PS	10.656	1.0695	PXE	2.908	1.0076	63.69

where I_s is the background corrected scattered intensity, I_w is the background corrected scattering from water, TRW is the transmission of water, TRS is the transmission of the sample, and d_s is the sample thickness. $g(\lambda)$ corrects the data for anisotropic scattering effects caused by inelastic scattering from the water.[14]

The normalized intensity was then analyzed by using the standard expression for small-angle scattering from a dilute solution of polymer 2 in polymer 1.[13]

$$K^*\frac{c_2}{I(q)} = \frac{1}{M_w}\left[1 + \frac{R_z^2q^2}{3}\right] + 2A_2c_2 \tag{2}$$

c_2, M_w, and R_z are the concentration in g/mL, the weight-average molecular weight, and the z-average radius of gyration of polymer 2, respectively. A_2 is the osmotic second virial coefficient for polymer 2 in polymer 1.

$$K^* = \left[b_2 - \frac{v_2}{v_1}b_1\right]^2\frac{N_A}{m_2^2} = K^2\frac{N_A}{m_2^2} \tag{3}$$

b_i and v_i are the neutron scattering length and molar volume of a segment of polymer i, respectively. A segment is taken to be a monomer of molecular weight m_i; N_A is Avogadro's number. Values of K^2, the neutron contrast, are listed in Table III together with the values of the specific volumes used in the calculations. The molar volumes of the deuterated polymers have been assumed to be the same as their hydrogenous analogues and have been calculated by using the expression

$$v_i^H = v_i^D = v_{i,sp}{}^H m_i^H$$

where v_i^H and v_i^D are the molar volumes of the hydrogenous and deuterated monomers of polymer i, respectively and, $v_{i,sp}{}^H$ and m_i^H are the specific volume of hydrogenous polymer i and its monomer molecular weight, respectively. All the values of the specific volumes were calculated by using the equations for the specific volume of a polymer melt from the paper of Zoller and Hoehn.[15] Since at all temperatures the blend is above its glass transition it was further assumed, when calculating K^2, that the d-PXE (in the blend) had a specific volume appropriate to that of a melt—not a glass—at all temperatures.

(2) Flory's Equation-of-State Theory. Flory's equation-of-state theory, including the entropy parameter Q_{12}, has the following state equation for the pure polymers and their mixtures. (All the equation-of-state symbols are defined in the Appendix.)

$$\frac{\tilde{P}\tilde{v}}{\tilde{T}} = \frac{\tilde{v}^{1/3}}{\tilde{v}^{1/3} - 1} - \frac{1}{\tilde{T}\tilde{v}} \tag{4}$$

Subscript 1 refers to component 1 (PS) and subscript 2 refers to component 2 (PXE). Parameters which have either no subscript or a subscript 12 refer to the blends. Hence, $i = 1, 2$

$$\tilde{v}_i = \left[\frac{3 + 4\alpha_iT}{3 + 3\alpha_iT}\right]^3 \tag{5}$$

$$\tilde{T}_i = \frac{\tilde{v}_i^{1/3} - 1}{\tilde{v}_i^{4/3}} = \frac{T}{T_i^*} \tag{6}$$

$$P_i^* = \gamma_iT\tilde{v}_i^2 \tag{7}$$

$$v_{i,sp}{}^* = v_{i,sp}/\tilde{v}_i \tag{8}$$

$$\Phi_2 = \frac{m_2v_{2,sp}{}^*}{m_1v_{1,sp}{}^* + m_2v_{2,sp}{}^*} \qquad \Phi_1 = 1 - \Phi_2 \tag{9}$$

$$\Theta_2 = \frac{(s_2/s_1)\Phi_2}{(s_2/s_1)\Phi_2 + \Phi_1} \qquad \Theta_1 = 1 - \Theta_2 \tag{10}$$

$$P^* = \Phi_1P_1{}^* + \Phi_2P_2{}^* - \Phi_1\Theta_2X_{12} \tag{11}$$

$$T^* = \frac{P^*}{\Phi_1P_1{}^*/T_1{}^* + \Phi_2P_2{}^*/T_2{}^*} \tag{12}$$

From eq 4–12 the excess thermodynamic quantities of the mixture can be derived; thus

$$\Delta H = v_{sp}{}^*[\Phi_1P_1{}^*/\tilde{v}_1 + \Phi_2P_2{}^*/\tilde{v}_2 - P^*/\tilde{v}] \tag{13}$$

and

$$TS^R = -3Tv_{sp}{}^*\left[\frac{\Phi_1P_1{}^*}{T_1{}^*}\ln\frac{\tilde{v}_1^{1/3} - 1}{\tilde{v}^{1/3} - 1} + \frac{\Phi_2P_2{}^*}{T_2{}^*}\ln\frac{\tilde{v}_2^{1/3} - 1}{\tilde{v}^{1/3} - 1} + \frac{1}{3}\Phi_1\Theta_2Q_{12}\right] \tag{14}$$

where

$$G^R = \Delta H - TS^R \tag{15}$$

The partial molar quantities of eq 13–15 are related to χ_H, χ_S, and χ_t, respectively. Thus

$$\Delta\bar{H}_1 = P_1{}^*V_1{}^*\left[(\tilde{v}_1{}^{-1} - \tilde{v}^{-1}) + \frac{\alpha T}{\tilde{v}}\frac{\tilde{T}_1 - \tilde{T}}{\tilde{T}}\right] + \frac{V_1{}^*X_{12}}{\tilde{v}}\Theta_2{}^2(1 + \alpha T) = RT\chi_H\Phi_2{}^2 \tag{16}$$

$$T\bar{S}_1{}^R = -P_1{}^*V_1{}^*\left[3\tilde{T}_1\ln\frac{\tilde{v}_1^{1/3} - 1}{\tilde{v}^{1/3} - 1} - \frac{\alpha T}{\tilde{v}}\frac{\tilde{T}_1 - \tilde{T}}{\tilde{T}}\right] + \frac{V_1{}^*\Theta_2{}^2}{\tilde{v}}(\alpha TX_{12} + T\tilde{v}Q_{12}) = -RT\chi_S\Phi_2{}^2 \tag{17}$$

and

$$\bar{G}_1^R = \Delta\mu_1^R = P_1^* V_1^* \left[3\tilde{T}_1 \ln \frac{\tilde{v}_1^{1/3} - 1}{\tilde{v}^{1/3} - 1} + \tilde{v}_1^{-1} - \tilde{v}^{-1} \right] + \frac{V_1^* \Theta_2^2}{\tilde{v}} (X_{12} - T\tilde{v}Q_{12}) \quad (18)$$

therefore, $\chi_t = \chi_H + \chi_S$.

The spinodal can be calculated by applying the condition $\partial(\Delta\mu_1)/\partial\Phi_2 = 0$ where

$$\Delta\mu_1 = \Delta\mu_1^{comb} + \Delta\mu_1^R \quad (19)$$

and the combinatorial chemical potential, $\Delta\mu_1^{comb}$, is obtained from the lattice model of the Flory–Huggins theory. The expression for the spinodal is

$$-\frac{1}{\Phi_1} + \left(1 - \frac{r_1}{r_2}\right) - \frac{P_1^* V_1^*}{RT_1^*}\left(\frac{\partial\tilde{v}}{\partial\Phi_2}\right)\left(\frac{1}{\tilde{v} - \tilde{v}^{2/3}}\right) + \frac{P_1^* V_1^*}{RT_{sp}}\left(\frac{\partial\tilde{v}}{\partial\Phi_2}\right)\frac{1}{\tilde{v}^2} + \frac{V_1^* X_{12}}{RT_{sp}}\frac{2\Theta_2^2\Theta_1}{\tilde{v}\Phi_2\Phi_2} - \frac{V_1^* X_{12}}{RT_{sp}}\frac{\Theta_2^2}{\tilde{v}^2}\left(\frac{\partial\tilde{v}}{\partial\Phi_2}\right) - \frac{V_1^* Q_{12}}{R}\frac{2\Theta_2^2\Theta_1}{\Phi_1\Phi_2} = 0 \quad (20)$$

where

$$\frac{\partial\tilde{v}}{\partial\Phi_2} = \frac{\frac{\partial\tilde{P}}{\partial\Phi_2} - \frac{\partial\tilde{T}}{\partial\Phi_2}\left(\frac{\tilde{P}}{\tilde{T}} + \frac{1}{\tilde{T}\tilde{v}^2}\right)}{\frac{2}{\tilde{v}^3} - \frac{\tilde{T}}{3\tilde{v}^{3/5}}\frac{(3\tilde{v}^{1/3} - 2)}{(\tilde{v}^{1/3} - 1)^2}} \quad (21)$$

$$\frac{\partial\tilde{P}}{\partial\Phi_2} = \frac{\tilde{P}}{P^*}\left[P_1^* - P_2^* - \Theta_2 X_{12}\left(1 - \frac{\Theta_1}{\Theta_2}\right)\right] \quad (22)$$

and

$$\frac{\partial\tilde{T}}{\partial\Phi_2} = \frac{\tilde{T}}{\tilde{P}}\frac{\partial\tilde{P}}{\partial\Phi_2} + \frac{T}{P^*}\left(\frac{P_2^*}{T_2^*} - \frac{P_1^*}{T_1^*}\right) \quad (23)$$

Full derivations of eq 4–23 are given elsewhere.[16]

Results and Discussion

The values of A_2, R_z, and M_w obtained from the SANS measurements are listed in Table IV. A typical Zimm plot for set A is shown in Figure 1. Measurements of d-PS in PS and d-PXE in PXE were carried out at only one concentration and A_2 was assumed to be zero for both mixtures. Using SANS it has been shown that in the bulk polymer the chains adopt their unperturbed configuration and A_2 is zero.[17,18] It was, therefore, assumed that bulk PXE would exhibit similar conformational behavior.

The values of A_2 for PXE in PS are large and positive, indicating that PS is a good solvent for PXE. As the temperature increases, A_2 decreases, showing decreasing solvent power and confirming the expected behavior for a high molecular weight polymer blend which exhibits lower critical solution temperature behavior. At a higher temperature (outside the range of the measurements) the blend should eventually phase separate. An indication of the temperature above which phase separation should occur has been obtained by extrapolation of A_2 to zero, as shown in Figure 2. For a solution of a polymer in a low molecular weight solvent the temperature at which A_2 goes to zero is the Θ temperature, Θ_L. At Θ_L the solution is pseudoideal, the chains should adopt an unperturbed configuration and above Θ_L a polymer of infinite molecular weight should come out of solution. Θ_L can be similarly defined for a polymer blend and for the system under investigation $\Theta_L = 345 \pm 55$ °C. Θ_L thus marks the lower bound for phase separation of the system PXE in PS (M_w = 34 000).

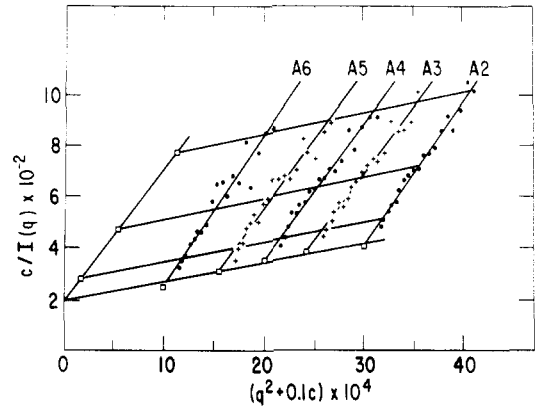

Figure 1. Zimm plot for d-PXE in PS measured at 128 °C. The notation A2–A6 refers to the mixtures listed in Table II.

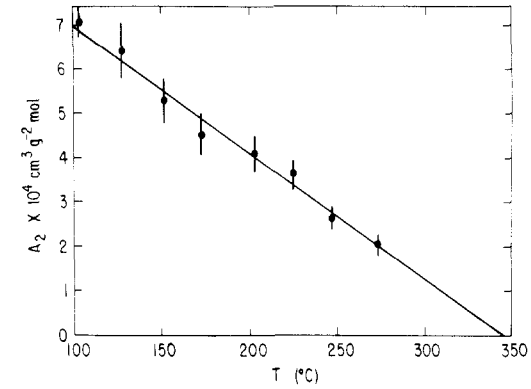

Figure 2. Temperature dependence of A_2 for the system d-PXE/PS. $\Theta_L = 345 \pm 55$ °C.

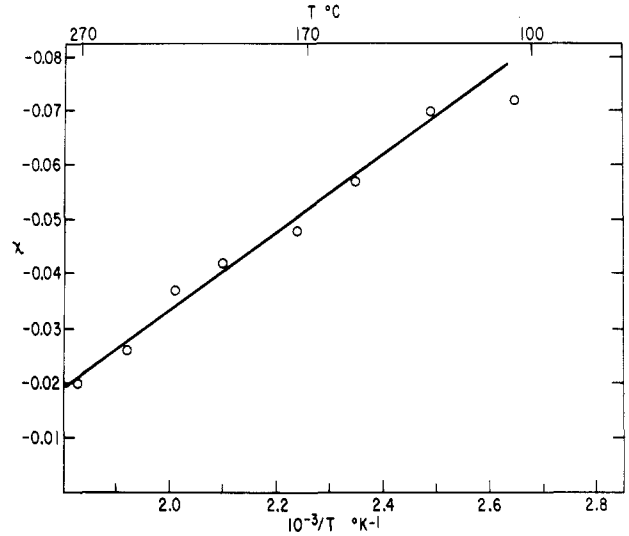

Figure 3. Dependence of χ_{12} on reciprocal temperature.

At infinite dilution the second virial coefficient A_2 is related to the Flory–Huggins interaction parameter, χ_{12}, in the following way:

$$\chi_{12} = \frac{1}{P_1}\left[\frac{1}{2} - \frac{V_1 M_2^2}{V_2^2} A_2\right] \quad (24)$$

where V_i, M_i, and P_i are the molar volume, molecular weight, and degree of polymerization of component i, respectively. Calculated values of χ_{12} for d-PXE in PS (Table IV) are displayed vs. reciprocal temperature in Figure 3. From the slope and intercept of the straight line

Table IV
Values of A_2, R_z, M_w^{SANS},[a] and χ_{12} from SANS Measurements[b]

sample	T, °C	10^4A_2, g^{-2} cm^3 mol	R_z, Å	$10^{-5}M_w$	$10^{-5}M_w^{SANS}$	χ_{12}
d-PXE/PXE			100.7	3.75	4.23	
d-PS/PS			51.1	3.33	2.92	
d-PS/PXE		2.74	53.1	3.33	3.76	−0.033
d-PXE/PS	104	7.05	85.4	3.75	3.49	−0.085
d-PXE/PS	128	6.39	86.0	3.75	3.29	−0.076
d-PXE/PS	152	5.27	86.6	3.75	3.56	−0.061
d-PXE/PS	173	4.5	88.6	3.75	3.53	−0.051
d-PXE/PS	203	4.10	90.6	3.75	3.60	−0.045
d-PXE/PS	225	3.64	89.2	3.75	3.81	−0.039
d-PXE/PS	247	2.63	92.5	3.75	3.93	−0.027
d-PXE/PS	273	2.06	91.7	3.75	3.71	−0.021

[a] M_w is listed for comparison. [b] Uncertainties are as follows: T, ±1 °C; 10^4A_2, ±10%; R_z, ±10%; $M_w^{SANS}10^{-5}$, ±10%; χ_{12}, ±30%.

fitted to the data, the partial molar heat and noncombinatorial entropy of mixing were derived, respectively. The values obtained, −170 cal/mol and −0.22 eu/mol, indicate that the favorable enthalpic driving force for mixing is partially negated by an unfavorable local entropic contribution: At 400 K, for example, the local entropic contribution negates about half of the heat of mixing.

If it is assumed that the partial molar heat of mixing is independent of composition, the integral heat produced by mixing 0.5 mol each of d-PXE and PS segments is calculable. The value obtained, −43 cal/mol, is identical with the −40 ± 10 cal/mol obtained by solution calorimetry.[9]

Although A_2 (and χ_{12}) varies quite markedly with temperature, the measured radius of gyration of d-PXE in PS is much less sensitive to temperature. The values of R_z are listed in Table IV. The value of R_z for d-PXE in PXE is greater than the values in PS. R_z also shows an unusual temperature dependence and appears to be increasing with increasing temperature, in contrast to the observed temperature dependence of A_2, which would appear to indicate a contracting chain. One possible explanation for the apparent decrease in R_z, when the matrix changes from PXE to PS, is that the PXE has degraded during the SANS experiments. The values of M_w measured by SANS are listed in Table IV. M_w is, within error, the same as that measured by low-angle light scattering for a sample of d-PXE which has not undergone the prolonged heat treatment.

Previous measurements of the unperturbed dimension of PXE have relied on extrapolation of good-solvent properties to those of a Θ solvent.[19] This method was used because PXE crystallizes from poor solvents before Θ conditions can be attained. Akers et al.[19] estimated an average value of $(r_0^2/M)^{1/2}$ of 0.85 for PXE, where r_0^2 is the mean-square unperturbed end-to-end distance. Assuming a Flory–Schultz distribution, R_z, at the Θ temperature, is estimated from this value of $(r_0^2/M)^{1/2}$ to be 84 Å. This compares with the value of 100 ± 10 Å for d-PXE in PXE measured by SANS. The value of M_w measured by SANS for d-PXE in PXE is 13% higher than the low-angle light scattering values whereas the error is estimated to be ±10%. This may mean that the measured R_z value is also high since R_z is calculated from the slope of $1/I$ vs. q^2 divided by the intercept which is proportional to $1/M$. Thus if M is large, R_z will decrease. However, although the apparent decrease in chain dimensions may not be real (it will be necessary to repeat the measurements to check), this does not eliminate the unusual temperature dependence. One possible explanation for the temperature dependence of R_z is to postulate a change in the conformation of PXE when it is mixed with PS brought about by the strong specific interactions between the polymers. This interaction will decrease in strength with increasing temperature and thus the conformation of the chain would change. In order to check this hypothesis it will be necessary to carry out further measurements particularly at high q values where changes in local conformation may be observed. At present it is impossible to say whether this increase in chain dimension with temperature is significant or not. The value of R_z measured for d-PS in PXE confirms previous results[8,20–22] and shows that PS is slightly expanded in PXE, the opposite effect to that which is observed for PXE in PS.

Table V
Values of α, γ, and v_{sp} Used in the Calculations at 250 °C

PS/PXE	$10^{-4}\alpha$, °C	γ, J cm^{-3} °C^{-1}	v_{sp}, cm^3 g^{-1}
1/0	6.1	0.6197	1.0715
0/1	7.38	0.644	1.0098
0.2/0.8	6.32		
0.4/0.6	6.556		
0.5/0.5	6.68		
0.6/0.4	6.81		
0.8/0.2	7.08		

In order to obtain more information about the interactions between the two polymers, equation-of-state theory has been applied to the blend. Values of the thermal expansion coefficient α, the thermal compressibility β_T, and the specific volume v_{sp} of the pure components and the blends at 250 °C were obtained from the paper of Zoller and Hoehn.[15] Values of the thermal pressure coefficient γ were calculated by using the expression $\gamma = \alpha/\beta_T$. α, γ, and v_{sp} used in the equation-of-state calculations are listed in Table V. To obtain values of α, γ, and v_{sp} at temperatures other than 250 °C, the following equations were used.[23]

$$\alpha = \alpha_0 + \alpha_0^2(7 + 4\alpha_0 T)\Delta T/3 \quad (25)$$

$$\gamma = \gamma_0 - \gamma_0(1 + 2\alpha_0 T)\Delta T/T \quad (26)$$

$$v_{sp} = v_{sp}^0 \exp(\alpha \Delta T) \quad (27)$$

s_2/s_1 for the blend was calculated by using Bondi's group contribution data[24] and a value of 1.1 was obtained.

Values of $\tilde{v}$, $\tilde{T}$, and P^* were calculated at 247 °C from eq 5, 6, and 12 with the data for α, γ, and v_{sp}, and with the P^* obtained, a value of X_{12} could be calculated from eq 11. X_{12} was calculated for a number of concentrations and, assuming it to be concentration independent, an average value was obtained at 247 °C of −4.9 J cm^{-3}. Knowing the value of χ_{12} from SANS and using eq 18 permitted the value of the entropy correction factor Q_{12} to be calculated as −0.0045 J cm^{-3} K^{-1}.

Using the measured values of A_2 at each temperature it is possible, in principle, to calculate $\bar{X}_{12}$, given by

$$\bar{X}_{12} = X_{12} - T\tilde{v}Q_{12} \quad (28)$$

However, to calculate $\bar{X}_{12}$ a value of $\tilde{v}$ is required at each temperature and composition to insert into eq 18. Al-

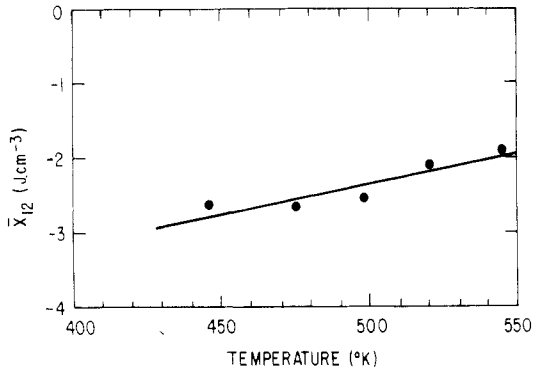

Figure 4. Plot of $\bar{X}_{12}$ vs. temperature. $\bar{X}_{12}$ was calculated by using the method described in the text. $X_{12} = -6.39$ and $Q_{12} = -0.0063$.

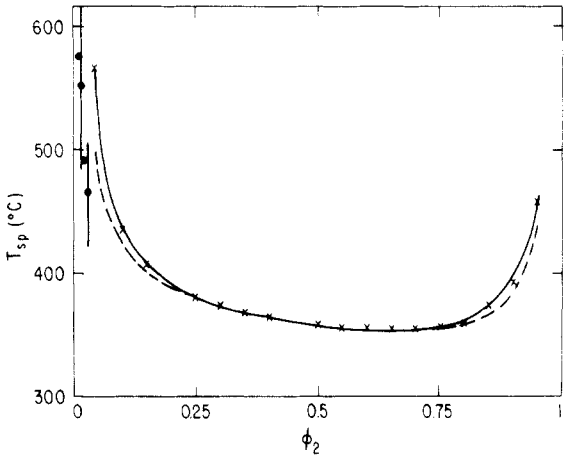

Figure 5. Spinodal for PS/PXE simulated by using eq 20; (—) $X_{12} = -4.90$ and $Q_{12} = -0.0045$; (---) $X_{12} = -6.39$ and $Q_{12} = -0.0063$. (●) measured T_{sp} from Figure 6.

though eq 25 has been used to calculate the expansion coefficient of the blend at 247 °C and thus $\tilde{v}$, for which ΔT is only 3 °C, it was not considered to be valid for temperatures far from 250 °C since the equation was derived for pure components.[23] Since the values of $\tilde{v}$ are not available, a method has been devised to calculate $\bar{X}_{12}$. A value of X_{12} was guessed and this value was fed into eq 11; thus P^*, T^*, and therefore $\tilde{v}$ could be calculated at a number of temperatures corresponding to the temperatures of the SANS measurements. X_{12} was assumed to be constant. The calculated values of $\tilde{v}$ were put into eq 18 and values of $\bar{X}_{12}$ were calculated. $\bar{X}_{12}$ was then plotted against temperature and values of X_{12} and Q_{12} were obtained (ignoring the small variation of $\tilde{v}$ with T in this equation). X_{12}, thus obtained, was then fed back into eq 11 and the whole process was repeated until the initial and final values of X_{12} were sufficiently close together. In this way it was possible to obtain constant values of X_{12} and Q_{12} which best fit the SANS data over the entire temperature range. The values obtained were $X_{12} = -6.39$ and $Q_{12} = -0.0063$. The final plot of $\bar{X}_{12}$ vs. temperature is shown in Figure 4 and is a fairly good straight line showing that the use of constant values for X_{12} and Q_{12} over this temperature range is a good approximation. We believe in general that for systems having specific interactions, dissociation of the interaction at higher temperatures will result in a reduction of both X_{12} and Q_{12}. However, over the temperature range of our measurements, which is well away from the phase separation temperature, constant values of X_{12} and Q_{12} appear to fit the data well.

In order to calculate the approximate position of the spinodal for this blend the values of X_{12} and Q_{12} at 247 °C were used in eq 20. The simulated spinodal is plotted in Figure 5. If the values of X_{12} and Q_{12} obtained from Figure 4 are used there is essentially no change in the calculated spinodal. The accuracy of the simulated spinodal will depend on the temperature dependence of X_{12} and Q_{12} at higher temperatures closer to the spinodal. Although we have no way of predicting the temperature dependence of X_{12} and Q_{12}, there is a method of checking the position of the spinodal using the SANS data.

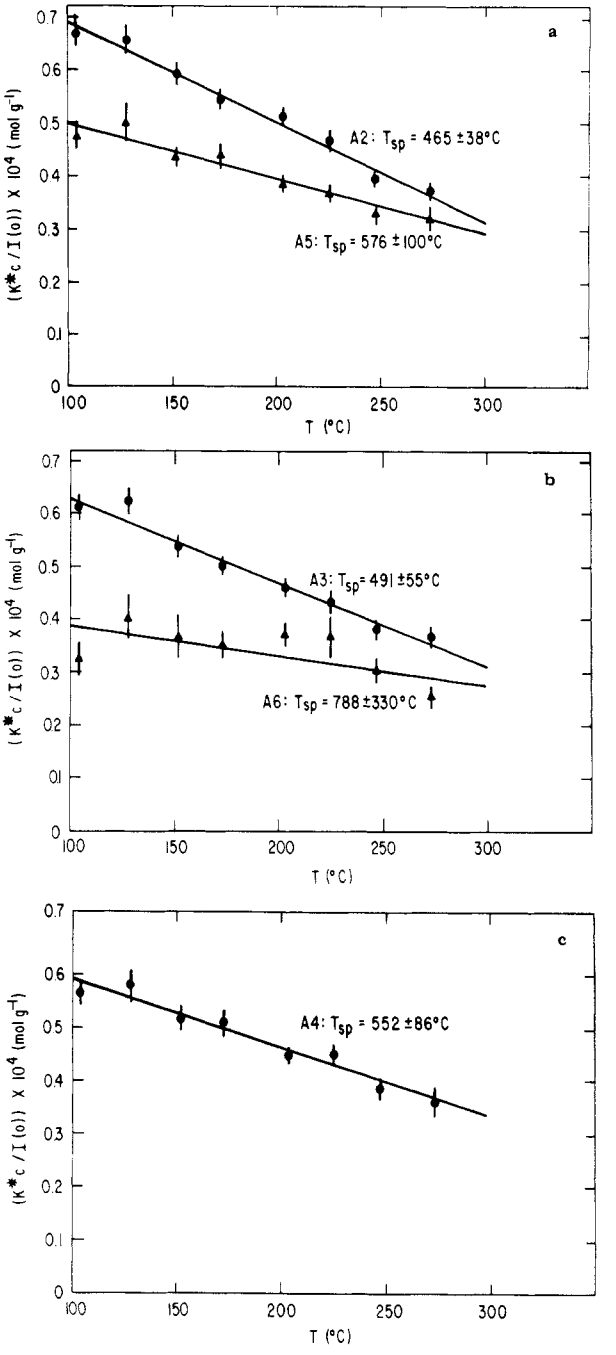

Figure 6. Plots of $K^*c/I(0)$ vs. temperature for different concentrations of d-PXE in PS. The values of T_{sp} obtained from these plots are shown in Figure 5. A2–A6 refer to the mixtures listed in Table II.

The definition of the spinodal is the condition where $\partial(\Delta\mu_1)/\partial\Phi_2 = 0$. The scattered intensity at $q = 0$, $I(0)$, is related to $\partial(\Delta\mu_1)/\partial\Phi_2$ in the following way:[25]

$$I(0) = \frac{KRTV_1\Phi_2}{\partial(\Delta\mu_1)/\partial\Phi_2} \tag{29}$$

where K is a constant. Therefore, at the spinodal the

intensity will tend to infinity or $I(0)^{-1}$ will tend to zero. The scattered intensity for each concentration of d-PXE in PS has been extrapolated to $q = 0$ and is plotted as $c/I(0)$ vs. T in Figure 6. A least-squares fit has been carried out on each of the sets of data and the values of the spinodal temperatures obtained are indicated on the figure. The spinodal temperatures obtained are plotted on Figure 5. The errors in the extrapolation in Figure 6 are large, particularly for the lowest concentration because of the long extrapolation. A much more accurate value of the spinodal would be obtained if the measurements had been made much closer to the phase boundary. However, the values obtained do give an indication of the position of the spinodal which is in remarkably good agreement with the position of the simulated spinodal, although the concentration range of the measurements is very limited.

Conclusions

Small-angle neutron scattering measurements have shown that the PS/PXE blends will exhibit a lower critical phase boundary in common with other high molecular weight polymer blends. Over the temperature range of the measurements the interaction parameter χ_{12} and both its enthalpic and entropic components are negative, indicating that the polymers are highly miscible. The enthalpic component is consistent with heats of mixing derived from calorimetric experiments. The Θ temperature for this system is predicted to be at 345 °C.

Equation-of-state calculations based on the experimental data have been used to simulate a spinodal for the system. The simulated spinodal curve predicts that phase separation should occur in a temperature range above 350 °C, and this is confirmed by the SANS measurements.

Acknowledgment. We thank Dr. J. S. Higgins for her comments on the paper and local contact Dr. A. Wright for his help with the experiments.

Appendix. List of Symbols Used in Equation-of-State Theory

G^R	residual Gibbs free energy
$\bar{G}_1^R$	partial molar residual Gibbs free energy of component 1
ΔH	enthalpy of mixing
$\Delta \bar{H}_1$	partial molar enthalpy of mixing of component 1
m_i	mass fraction of component i
N_A	Avogadro's number
$\tilde{P}_i$	reduced pressure of species i
P_i^*	hard-core pressure of species i
$\tilde{P}$	reduced pressure of the mixture
P^*	hard-core pressure of the mixture
Q_{12}	interaction entropy parameter
r_i	chain length of species i
R	gas constant
s_i	segment surface area per unit volume of component i
S^R	residual entropy of mixing
$\bar{S}_1^R$	partial molar residual entropy of mixing of component 1
T	temperature
$\tilde{T}_i$	reduced temperature of species i
T_i^*	hard-core temperature of species i
$\tilde{T}$	reduced temperature of the mixture
T^*	hard-core temperature of the mixture
T_{sp}	spinodal temperature
V_1^*	molar hard-core volume of component 1
$\tilde{v}_i$	reduced volume of component i
$\tilde{v}$	reduced volume of the mixture
$v_{i,sp}^*$	hard-core specific volume of component i
$v_{i,sp}$	specific volume of component i
X_{12}	interaction parameter term
α_i	thermal expansion coefficient of component i
α	thermal expansion coefficient of the mixture
γ_i	thermal pressure coefficient of component i
Φ_i	volume fraction of species i
Θ_i	site fraction of species i
$\Delta\mu_1$	chemical potential of component 1
$\Delta\mu_1^R$	residual chemical potential of component 1
$\Delta\mu_i^{comb}$	combinatorial chemical potential of component 1
χ_H	enthalpic interaction parameter
χ_S	entropic interaction parameter
χ_t	total interaction parameter

References and Notes

(1) See, for example: Olabisi, O.; Robeson, L. M.; Shaw, M. T. "Polymer–Polymer Miscibility"; Academic Press: New York, 1979.
(2) Stoelting, J.; Karasz, F. E.; MacKnight, W. J. *Polym. Eng. Sci.* **1970**, *10*, 133.
(3) (a) Wellinghof, S. T.; Koenig, J. L.; Baer, E. *J. Polym. Sci., Polym. Phys. Ed.* **1977**, *15*, 1913. (b) Lefebvre, D.; Jasse, B.; Monnerie, L. *Polymer* **1981**, *22*, 1616.
(4) Shultz, A. R.; Beach, B. M. *Macromolecules* **1974**, *7*, 902.
(5) Vukovic, R.; Karasz, F. E.; MacKnight, W. J. *J. Appl. Polym. Sci.* **1983**, *28*, 219.
(6) Fried, J. R.; Karasz, F. E.; MacKnight, W. J. *Macromolecules* **1978**, *11*, 150.
(7) Kambour, R. P.; Bendler, J. T.; Bopp, R. C. *Macromolecules* **1983**, *16*, 753.
(8) Maconnachie, A.; Kambour, R. P.; Bopp, R. C. *Polymer* **1984**, *22*, 357.
(9) Weeks, N. E.; Karasz, F. E.; MacKnight, W. J. *J. Appl. Phys.* **1977**, *48*, 4068.
(10) Yee, A. F. *Polym. Eng. Sci.* **1977**, *17*, 213.
(11) Djordjevic, M. B.; Porter, R. S. *Polym. Eng. Sci.* **1983**, *23*, 650.
(12) White, D. M.; Nye, S. A. *Macromolecules*, preceding paper in this issue.
(13) Maconnachie, A.; Richards, R. W. *Polymer* **1978**, *19*, 739.
(14) May, R. P.; Ibel, K.; Haas, J. *J. Appl. Crystallogr.* **1982**, *15*, 15.
(15) Zoller, P.; Hoehn, H. H. *J. Polym. Sci., Polym. Phys. Ed.* **1982**, *20*, 1385.
(16) Rostami, S. Ph.D. thesis, Imperial College, 1983.
(17) Cotton, J. P.; Decker, D.; Benoit, H.; Farnoux, B.; Higgins, J.; Jannink, G.; Ober, R.; Picot, C.; des Cloizeaux, J. *Macromolecules* **1974**, *7*, 863.
(18) Schelten, J.; Kruse, W. A.; Kirste, R. G. *Kolloid Z. Z. Polym.* **1973**, *251*, 919.
(19) Akers, P. J.; Allen, G.; Bethell, M. J. *Polymer* **1968**, *9*, 575.
(20) Kambour, R. P.; Bopp, R. C.; Maconnachie, A.; MacKnight, W. J. *Polymer* **1980**, *21*, 133.
(21) Wignall, G. D.; Child, H. R.; Li-Aravena, F. *Polymer* **1980**, *21*, 131.
(22) Schmitt, B. J.; Kirste, R. G.; Jelenic, J. *Makromol. Chem.* **1979**, *181*, 1655.
(23) Zhikuan, Chai; Ruona, Sun; Walsh, D. J.; Higgins, J. S. *Polymer* **1983**, *24*, 263.
(24) Bondi, A. *J. Phys. Chem.* **1964**, *68*, 44.
(25) Flory, P. J. "Principles of Polymer Chemistry"; Cornell University Press: Ithaca, NY, 1953.